University of Leeds
School of Electronic and Electrical Engineering

ELEC5333M - Wireless Communication System Design

Group Lab Report

Student: Harry Carless - 201508537
Student: Rahul Verma - XXXXXXXXX
Student: Marima Yoo - XXXXXXXXX

Module Leader: Dr Nutapong Somjit

1 Introduction

This report presents the work carried out across five simulation-based laboratories using Keysight ADS, each examining a different subsystem within a wireless communication link. Together, these studies explore how theoretical concepts introduced in the module appear in practical design scenarios, and how subsystem behaviour influences overall system performance.

The laboratories cover core RF functions including link budgeting, amplifier linearity, filtering, transistor operation and antenna radiation. For each task, simulations are used not only to obtain quantitative results but to interpret them in the context of the underlying theory. This approach allows the accuracy and limitations of the models to be assessed, and highlights how design choices at one stage can constrain or improve the behaviour of the complete link.

The purpose of the report is therefore twofold: to document the simulation methods and key findings from each laboratory, and to form a coherent view of how these individual results connect to broader wireless system design. The following sections outline the methodology, present and discuss the main results, and reflect on the implications for real RF subsystem design.

2 Link Budget and Propagation (Lab 1)

This laboratory applies link-budget equations to predict received power from transmit power, antenna gains and propagation loss, then validates the predictions in ADS. The results highlight how frequency, distance and additional attenuation terms shape link performance and motivate the later labs.

The theoretical background draws on the Friis transmission relationship and the free–space path loss model, which describe how power decays with distance and frequency. Received power is obtained by combining transmitter power, antenna gains and propagation loss in decibel form. Antenna directivity is central, with higher frequency systems relying on significant antenna gain to counter increased path loss. Free–space propagation assumes an unobstructed line–of–sight link, providing a controlled baseline for analysis. ADS then allows this ideal behaviour to be compared against scenarios that include additional losses such as atmospheric absorption or building penetration.
Before validating the system performance using ADS, each scenario was first evaluated using the link-budget equations provided in the Lab 1 handbook [**?**]. The received power is obtained using:

$$P_r(dBm) = P_t(dBm) + G_t(dBi) + G_r(dBi) + 20\log_{10}\left(\frac{\lambda}{4\pi R}\right),$$

with antenna gains and parabolic reflector diameters calculated using:

$$G_x(dBi) = 10\log_{10}\left(\eta\frac{\pi^2 d^2}{\lambda^2}\right).$$

These expressions provide a baseline prediction for each wireless link prior to introducing simulation tools or additional channel impairments.

Exercise A: 700 MHz Terrestrial Broadcast Link

For a carrier frequency of 700 MHz, the wavelength is:

$$\lambda = \frac{c}{f} = \frac{3\times10^8}{700\times10^6} = 0.43 \text{ m}.$$

The transmit power of 5 kW corresponds to

$$P_t = 10\log_{10}(5\times10^6) = 66.99 \text{ dBm}.$$

The free-space loss over 25 km is

$$\text{FSPL} = 20\log_{10}\left(\frac{0.43}{4\pi\cdot25\times10^3}\right) = -117.30 \text{ dB}.$$

The received power is therefore

$$P_r = 66.99 + 3 + 10 - 117.30 = -37.31 \text{ dBm}.$$

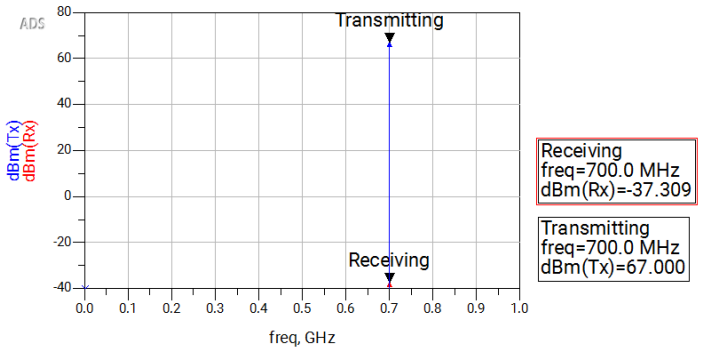

Figure 1: Simulated received-power results for Lab 1 Exercise A.

Exercise B: 38 GHz Backbone Link

In this exercise, the objective is to determine the diameter of the transmit parabolic antenna required to achieve a received power of $-50\,\text{dBm}$. The carrier frequency is 38 GHz, giving a wavelength of

$$\lambda = \frac{c}{f} = \frac{3 \times 10^8}{38 \times 10^9} = 7.89 \times 10^{-3}\ \text{m}.$$

The receiver uses a 15 cm dish with efficiency $\eta = 0.55$. Its gain is

$$G_r = 10\log_{10}\left(\eta\frac{\pi^2 d_r^2}{\lambda^2}\right) = 10\log_{10}\left(0.55\frac{\pi^2(0.15)^2}{(7.89\times10^{-3})^2}\right) = 32.92\ \text{dBi}.$$

The free–space loss over $R = 10\,\text{km}$ is

$$\text{FSPL} = 20\log_{10}\left(\frac{\lambda}{4\pi R}\right) = -144.04\ \text{dB}.$$

Atmospheric absorption adds a further 10 dB attenuation. The system transmit power is 100 mW, corresponding to

$$P_t = 10\log_{10}(100) = 20\ \text{dBm}.$$

The link budget expression becomes

$$P_r = P_t + G_t + G_r + \text{FSPL} - 10.$$

Setting the target received power $P_r = -50\,\text{dBm}$ and solving for G_t gives

$$-50 = 20 + G_t + 32.92 - 144.04 - 10,$$

$$-50 = -101.12 + G_t,$$

$$G_t = 51.12\ \text{dBi}.$$

The corresponding transmit-antenna diameter follows from the parabolic reflector gain expression:

$$G_t = 10\log_{10}\left(\eta\frac{\pi^2 d_t^2}{\lambda^2}\right),$$

$$d_t = \lambda\sqrt{\frac{10^{G_t/10}}{\eta\pi^2}}.$$

Substituting $\eta = 0.55$, $\lambda = 7.89\times10^{-3}\,\text{m}$ and $G_t = 51.12\,\text{dBi}$,

$$d_t = 7.89\times10^{-3}\sqrt{\frac{10^{5.112}}{0.55\pi^2}} = 1.22\ \text{m}.$$

Thus, a transmit-antenna diameter of approximately **1.22 m** is required to achieve a received power of $-50\,\text{dBm}$ under the stated conditions.

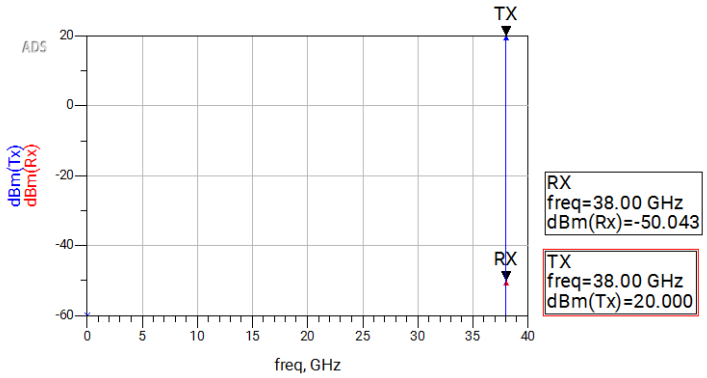

Figure 2: Simulation results for the 38 GHz backbone link (Exercise B). The simulated received power of -50.04 dBm matches the analytical prediction.

Atmospheric attenuation varies with frequency due to absorption by oxygen and water vapour, producing alternating low–loss transmission windows and high–loss absorption bands (see Fig. 3). The 38 GHz region falls within a relatively favourable window, whereas frequencies near 22 GHz and 60 GHz exhibit significantly greater loss. [1] The 10 dB attenuation term used in this exercise therefore represents a single point on a broader frequency–dependent profile and illustrates the importance of accounting for atmospheric absorption in long–distance link design.

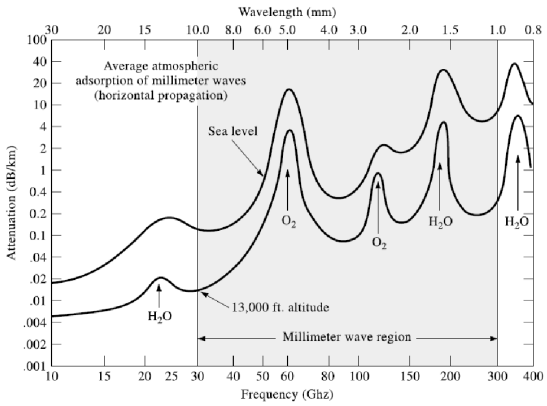

Figure 3: Atmospheric attenuation vs frequency, showing absorption features from oxygen and water vapour [2].

Exercise C: 1.8 GHz Cellular Link

In exercise C, further attenuation factors such as fading margin and building penetration loss are considered within the link budget. For a 1.8 GHz carrier:

$$\lambda = \frac{3 \times 10^8}{1.8 \times 10^9} = 0.167 \text{ m}.$$

The transmitter radiates 100 W, corresponding to

$$P_t = 10 \log_{10}(100\,\text{W}/1\,\text{mW}) = 10 \log_{10}(10^5) = 50 \text{ dBm}.$$

The free–space path loss over a 5 km link is

$$\text{FSPL} = 20 \log_{10}\left(\frac{\lambda}{4\pi R}\right) = 20 \log_{10}\left(\frac{0.167}{4\pi \cdot 5000}\right) = -111.53 \text{ dB}.$$

The transmitter antenna gain is $G_t = 6$ dB and the receiver antenna gain is $G_r = 0$ dB. Fading margin (20 dB) and building penetration loss (6 dB) combine to give a total additional attenuation of

$$L_{\text{extra}} = 20 + 6 = 26 \text{ dB}.$$

The received power is therefore

$$P_r = P_t + G_t + G_r + \text{FSPL} - L_{\text{extra}},$$

$$P_r = 50 + 6 + 0 - 111.53 - 26,$$
$$P_r = -81.53 \text{ dBm}.$$

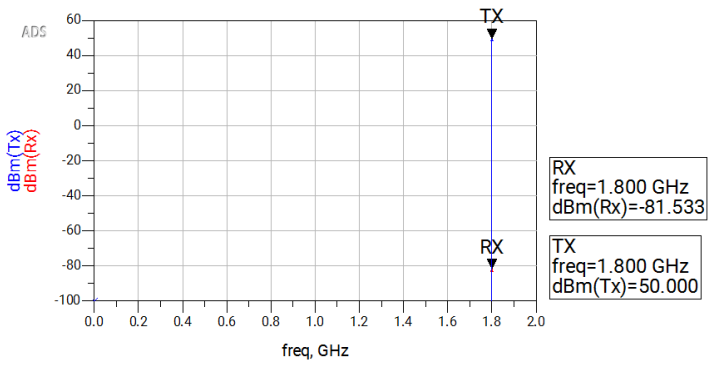

Figure 4: Simulation results for the 1.8 GHz cellular link (Exercise C). The simulated value of $P_r = -81.53$ dBm matches the analytic calculation.

Exercise D: Satellite TV Downlink

The received IF power for a satellite TV system is calculated using the link parameters provided. The transmit frequency is 12 GHz, giving a wavelength

$$\lambda = \frac{3 \times 10^8}{12 \times 10^9} = 0.025 \text{ m}.$$

The spacecraft radiates 100 W, corresponding to a transmit power

$$P_t = 10 \log_{10}(100 \text{ W}/1 \text{ mW}) = 50 \text{ dBm}.$$

Both transmit and receive antennas have an efficiency of $\eta = 0.6$. The transmit antenna diameter is $d_t = 2$ m, giving

$$G_t = 10 \log_{10}\left(\eta \frac{\pi^2 d_t^2}{\lambda^2}\right) = 10 \log_{10}\left(0.6 \frac{\pi^2 (2)^2}{(0.025)^2}\right) = 45.79 \text{ dBi}.$$

The receive antenna diameter is $d_r = 0.6$ m:

$$G_r = 10 \log_{10}\left(0.6 \frac{\pi^2 (0.6)^2}{(0.025)^2}\right) = 35.33 \text{ dBi}.$$

The free–space path loss (FSPL) for a geostationary satellite at 40 000 km is

$$\text{FSPL} = 20 \log_{10}\left(\frac{\lambda}{4\pi R}\right) = 20 \log_{10}\left(\frac{0.025}{4\pi \cdot 40\,000 \times 10^3}\right) = -206.10 \text{ dB}.$$

Atmospheric absorption produces a further 2 dB attenuation. After the receive antenna, the signal is amplified by a low-noise amplifier (LNA) with 30 dB gain and downconverted in a mixer with a 10 dB conversion loss.
The total received IF power is therefore

$$P_{\text{IF}} = P_t + G_t + G_r + \text{FSPL} - 2 \text{ dB} + 30 \text{ dB} - 10 \text{ dB},$$
$$P_{\text{IF}} = 50 + 45.79 + 35.33 - 206.10 - 2 + 30 - 10,$$
$$P_{\text{IF}} = -56.98 \text{ dBm}.$$

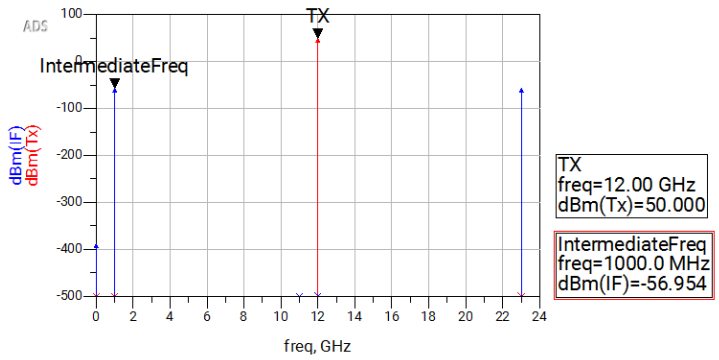

Figure 5: Simulation showing IF power of approximately $-56.95\,\text{dBm}$ for the satellite TV downlink (Exercise D). The calculated IF power of $-56.98\,\text{dBm}$ agrees with the simulated value.

Discussion of Lab 1

3 Amplifier Linearity and Intermodulation (Lab 2)

Exercise 2A: Second–order intermodulation products

A weakly nonlinear device may be written as $y = a_1x + a_2x^2 + a_3x^3 + \ldots$. For a two–tone input $x = A(\cos\omega_1 t + \cos\omega_2 t)$, the a_2x^2 term generates components at $f_1 \pm f_2$. The fundamental power scales as A^2 while IM2 power scales as A^4, giving a 2:1 slope on a dB input–output plot.
The IM2 extrapolation is $P_{\text{IM2}} = 2P_{\text{in}} + C_2$. At the intercept point, $IP2 = 2IP2 + C_2$, hence $C_2 = -IP2$. Expressing the IM2 level in terms of the fundamental output P_0 gives

$$P_{\text{IM2}} = 2P_0 - IP2.$$

Exercise 2B: Third–order intermodulation products

The cubic term produces the IM3 tones at $2f_1 \pm f_2$ and $2f_2 \pm f_1$. Here the IM3 amplitude scales as A^3, so IM3 power scales as A^6, resulting in a 3:1 slope.
Using $P_{\text{IM3}} = 3P_{\text{in}} + C_3$ and the intercept condition $IP3 = 3IP3 + C_3$ gives $C_3 = -2IP3$. Hence,

$$P_{\text{IM3}} = 3P_0 - 2IP3.$$

Exercise 2C: Two–tone distortion analysis

Two tones at $f_1 = 900\,\text{MHz}$ and $f_2 = 950\,\text{MHz}$, each at $-10\,\text{dBm}$, drive an amplifier with $G = 20\,\text{dB}$, $IP2 = 25\,\text{dBm}$, $IP3 = 30\,\text{dBm}$. The fundamentals at the output are

$$P_0 = -10 + 20 = 10\ \text{dBm}.$$

Second–order products: Frequencies: $f_2 - f_1 = 50\,\text{MHz}$ and $f_1 + f_2 = 1850\,\text{MHz}$. Power:

$$P_{\text{IM2}} = 2P_0 - IP2 = 20 - 25 = -5\ \text{dBm}.$$

Third–order products: Frequencies: $2f_1 - f_2 = 850\,\text{MHz}$, $2f_2 - f_1 = 1000\,\text{MHz}$. Power:

$$P_{\text{IM3}} = 3P_0 - 2IP3 = 30 - 60 = -30\ \text{dBm}.$$

Product	Frequency (MHz)	Power (dBm)
Fundamentals	900, 950	10
IM2 (diff / sum)	50, 1850	-5
Harmonics	1800, 1900	-11
IM3 (lower / upper)	850, 1000	-30
Higher IM3	2700–2850	-30 to -39

Table 1: Calculated IM2 and IM3 distortion products.

Comparison with ADS simulation. The ADS spectrum shows IM2 tones at −5 dBm and IM3 tones clustered around −30 dBm, matching theoretical predictions. Higher–frequency IM3 components appear weaker due to amplifier roll–off.

Practical significance. IM2 products generally fall far from the wanted band and can be filtered, whereas IM3 products lie close to the desired signals and therefore dominate linearity requirements, adjacent–channel interference and blocking behaviour. This is why IP3 is the primary figure of merit for RF amplifier linearity.

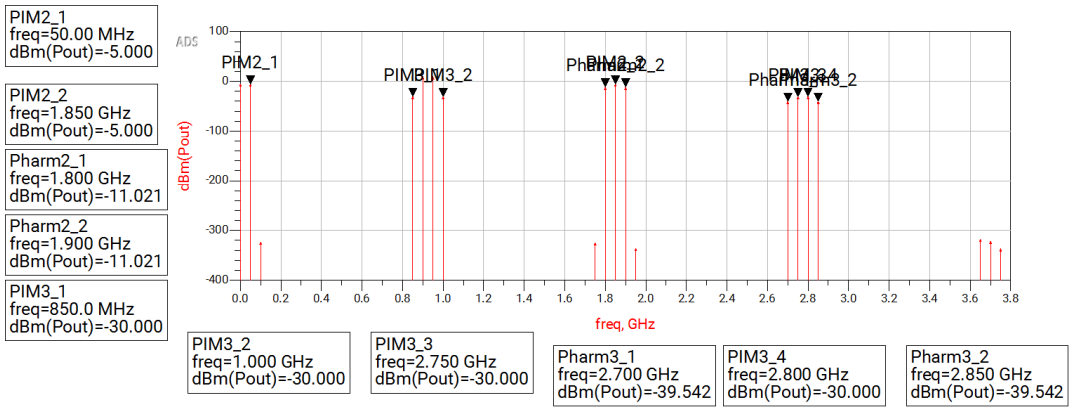

Figure 6: ADS output spectrum for the two–tone test, showing fundamental, IM2 and IM3 components.

Exercise B (Q2): LNA two–tone IM3 products

A low-noise amplifier (LNA) with gain $G = 30$ dB and input third–order intercept point $IIP3 = +5$ dBm is driven by two equal tones at $f_1 = 1.9$ GHz and $f_2 = 2.1$ GHz, each with input power $P_{\text{in}} = -10$ dBm. The corresponding output intercept point is

$$OIP3 = IIP3 + G = 5 + 30 = 35 \text{ dBm}.$$

The amplified fundamentals at the output are

$$P_0 = P_{\text{in}} + G = -10 + 30 = 20 \text{ dBm}.$$

IM3 frequencies. Third–order intermodulation products occur at the near-band frequencies

$$2f_1 - f_2 = 1.7 \text{ GHz}, \qquad 2f_2 - f_1 = 2.3 \text{ GHz},$$

with additional high-frequency components at $2f_1 + f_2 = 5.9$ GHz and $2f_2 + f_1 = 6.1$ GHz.

IM3 power levels. Using the output-referred relation

$$P_{\text{IM3}} = 3P_0 - 2OIP3,$$

gives

$$P_{\text{IM3}} = 3(20) - 2(35) = -10 \text{ dBm}.$$

Thus each IM3 product is predicted to appear at about −10 dBm at the LNA output.

Comparison with ADS simulation. The ADS spectrum in Fig. 7 shows IM3 tones at 1.7 and 2.3 GHz close to the predicted level, with any residual discrepancy attributable to device roll-off and filtering around the 100 MHz receiver bandwidth.

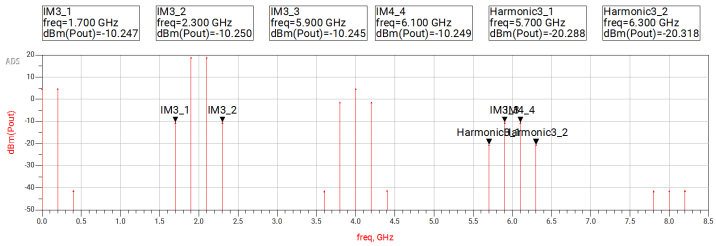

Figure 7: ADS two–tone spectrum for Exercise B (Q2).

Exercise C (Q3): Cascaded receiver linearity

The receiver chain consists of an RF filter, amplifier (Amp1), mixer and IF filter. The gains, noise figures and IIP3 values are given in the table in the question. First, output intercept points are found using $OIP3_i = IIP3_i + G_i$:

Stage	G_i (dB)	$OIP3_i$ (dBm)
RF filter	-1	98
Amp1	20	10
Mixer	-6	0
IF filter	-1	98

The corresponding linear gains are

$$G_1 = 0.79, \quad G_2 = 100, \quad G_3 = 0.25, \quad G_4 = 0.79,$$

giving a total gain of

$$G_{\text{tot}} = -1 + 20 - 6 - 1 = 12 \text{ dB}.$$

Cascaded OIP3. Using the output-referred cascade formula

$$\frac{1}{OIP3_{\text{cas}}} = \frac{1}{G_2G_3G_4\,OIP3_1} \frac{1}{G_3G_4\,OIP3_2} \frac{1}{G_4\,OIP3_3} \frac{1}{OIP3_4},$$

with $OIP3_1 = OIP3_4 \approx 6.31 \times 10^9$ mW, $OIP3_2 = 10$ mW and $OIP3_3 = 1$ mW, yields

$$OIP3_{\text{cas}} \approx 0.564 \text{ mW} \;\Rightarrow\; OIP3_{\text{cas}} \approx -2.47 \text{ dBm}.$$

With two input tones at $f_1 = 1.6$ GHz and $f_2 = 2.0$ GHz, each at -45 dBm, the output fundamentals are

$$P_0 = -45 + 12 = -33 \text{ dBm}.$$

The predicted IM3 level is therefore

$$P_{\text{IM3}} = 3P_0 - 2OIP3_{\text{cas}} = 3(-33) - 2(-2.47) = -94.1 \text{ dBm}.$$

IM3 frequencies and practical significance. The third–order products occur at

$$2f_1 - f_2 = 1.2 \text{ GHz}, \qquad 2f_2 - f_1 = 2.4 \text{ GHz}.$$

Although these fall outside the 1.6–2.0 GHz IF band and are attenuated by the IF filter, they indicate the receiver's sensitivity to strong adjacent tones. The cascaded OIP3 is dominated by the mixer and Amp1 stages, so improving either stage yields the largest system-level linearity benefit.

Comparison with ADS simulation. The ADS spectrum in Fig. 8 shows IM3 products at the same frequencies and close to the predicted level, confirming the cascade model.

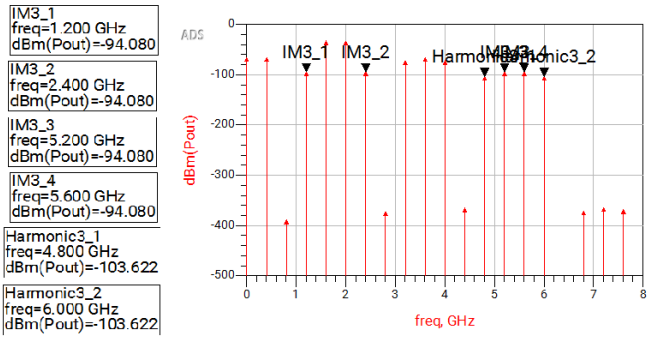

Figure 8: ADS two–tone spectrum for Exercise C (Q3).

4 Filter Behaviour (Lab 3)

Exercise 1: Three–pole Chebyshev lowpass filter

A third–order Chebyshev lowpass filter was synthesised with $F_p = 1$ GHz, $F_s = 3.2$ GHz, $A_p = 0.1$ dB and $A_s = 20$ dB for a 50 Ω source/load. The initial lumped LC prototype was then transformed to an equivalent transmission–line network and finally to a microstrip implementation on the specified substrate. Fig. 9 summarises each topology alongside its simulated response.

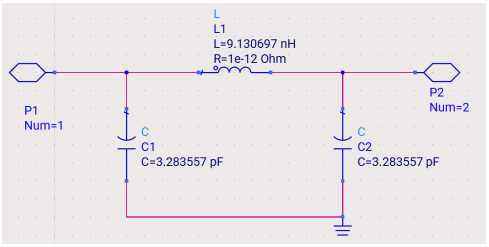

(a) LC prototype.

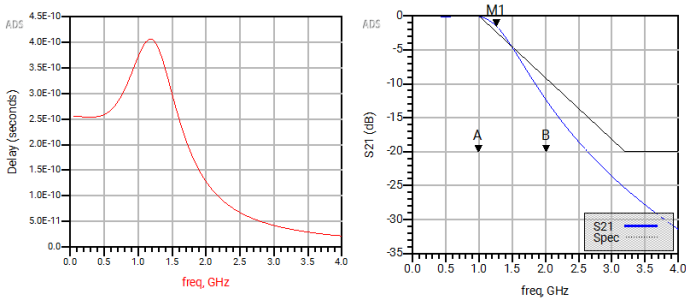

(b) LC response.

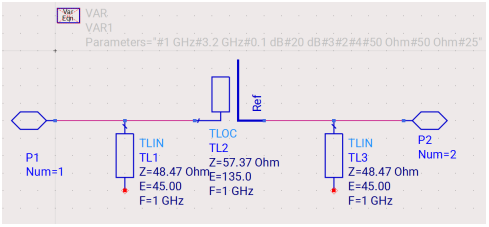

(c) TLine transformation.

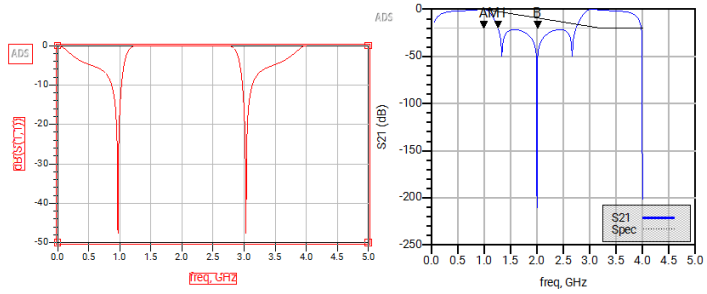

(d) TLine response.

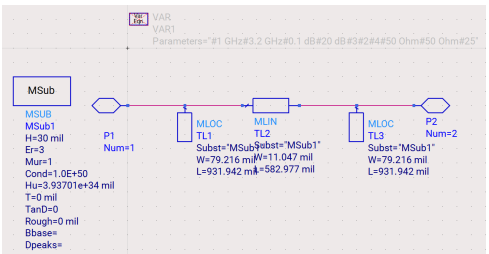

(e) Microstrip layout.

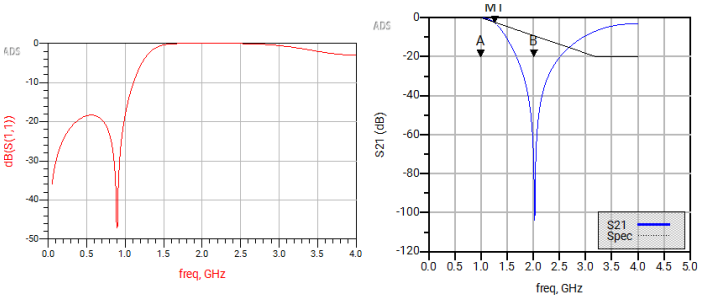

(f) Microstrip response.

Figure 9: Exercise 1 lowpass filter topologies and corresponding simulated S-parameters.

All three implementations meet the 0.1 dB passband ripple near 1 GHz and achieve at least 20 dB

attenuation by 3.2 GHz. The TLine and microstrip versions show slightly increased loss and a small shift of the stopband edge due to distributed effects and substrate dispersion, but preserve the intended Chebyshev shape.

Exercise 2: Microstrip Chebyshev bandpass filter

A microstrip Chebyshev bandpass filter was designed with $F_0 = 12$ GHz, $\Delta f = 1.3$ GHz and 0.1 dB passband ripple, targeting 30 dB rejection between 9 and 15 GHz. Fig. 10 shows the ADS lumped prototype and the resulting microstrip realisation after substrate parameterisation.

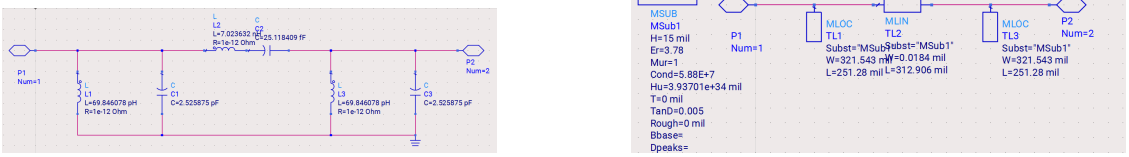

(a) Lumped prototype. **(b)** Microstrip realisation.

Figure 10: Bandpass filter circuits before and after microstrip conversion.

The return loss and insertion loss of the microstrip bandpass filter are shown in Fig. 11. The passband is centred close to 12 GHz with approximately 1.3 GHz 3 dB bandwidth, and S_{11} remains below -16 dB through most of the passband, consistent with the 0.1 dB ripple specification. Outside the band, the response rolls off rapidly and exceeds 30 dB attenuation across the 9–15 GHz stop region.

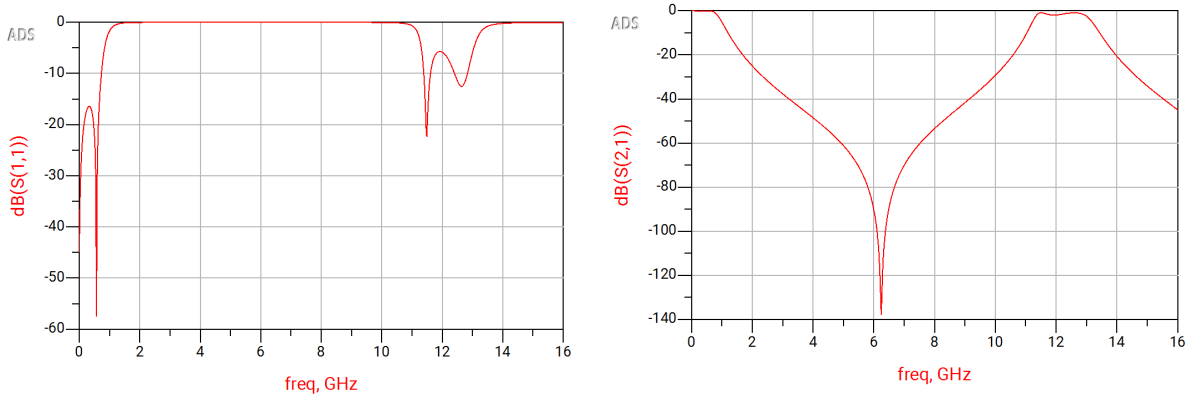

(a) Return loss S_{11}. **(b)** Insertion loss S_{21}.

Figure 11: Microstrip bandpass filter S-parameters.

5 Transistor Characteristics (Lab 4)

Exercise 1: DC bias and small-signal parameters

The BJT is modelled with $V_{BE} = 0.7$ V and $\beta = 100$. For each bias configuration, Kirchhoff's voltage law gives the base current, from which $I_C = \beta I_B$, $I_E = I_C + I_B$ and V_{CE} follow. ADS DC operating-point results are summarised in Table 2.

Circuit	I_B (A)	I_C (A)	I_E (A)	V_{BE} (V)	V_{CE} (V)	β
(a)	7.94×10^{-5}	8.0×10^{-3}	8.0×10^{-3}	0.822	4.056	100
(b)	2.28×10^{-5}	2.0×10^{-3}	2.0×10^{-3}	0.790	7.424	100

Table 2: ADS DC operating-point results for Exercise 1 circuits (a) and (b).

For circuit (a) the base current is $I_B \approx 7.94 \times 10^{-5}$ A, giving $I_C \approx 8$ mA and $V_{CE} \approx 4.06$ V. Circuit (b) introduces emitter degeneration, reducing the bias currents to $I_B \approx 2.28 \times 10^{-5}$ A, $I_C \approx 2$ mA and increasing the collector–emitter voltage to $V_{CE} \approx 7.42$ V. The simulated values are consistent with the hand calculations and show how emitter resistance improves bias stability at the cost of gain.

Exercise 2: Output characteristics

Using the Agilent HBT model, V_{CE} was swept from 0 to 5 V while stepping I_B from 20 to 200 μA. The resulting I_C–V_{CE} family is shown in Fig. 12.

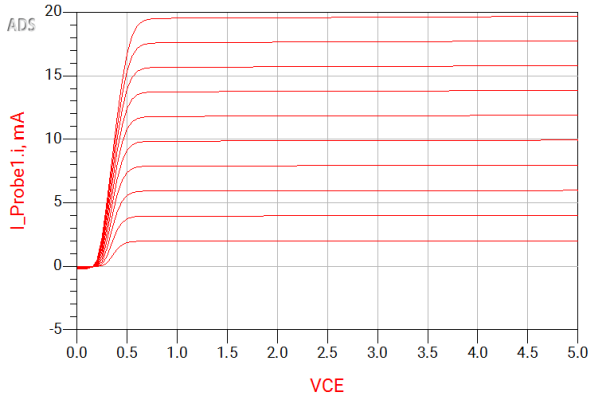

Figure 12: Collector current versus V_{CE} for stepped base currents.

Each curve exhibits a low-V_{CE} saturation region followed by a nearly flat active region where I_C is set by I_B. The slight upward slope in the active region indicates finite output resistance (Early effect), so I_C increases modestly with V_{CE}. Higher I_B shifts the curves upward approximately linearly, matching the expected proportionality between I_C and base drive.

Exercise 3: Frequency-dependent gain

The NPN device was replaced by the HBT model and the small-signal voltage gain was evaluated from 1 to 10 GHz. Fig. 13 shows the ADS AC results and derived parameters.

Figure 13: ADS AC gain magnitude/phase and extracted bias values.

The key values extracted from ADS are listed in Table 3.

f (GHz)	$\lvert A_v \rvert$	$\angle A_v$ (deg)
DC operating point		
$I_B = 3.953 \times 10^{-5}$ A	$I_C = 4.0 \times 10^{-3}$ A	$V_{CE} = -29.53$ V
AC gain versus frequency		
1.0	26.924	155.852
2.0	18.515	124.852
3.0	13.411	110.292
4.0	10.405	101.365
5.0	8.480	94.953
6.0	7.157	89.872
7.0	6.198	85.584
8.0	5.473	81.811
9.0	4.908	78.398
10.0	4.457	75.250

Table 3: ADS-derived DC bias currents/voltage and small-signal gain for Exercise 3.

The voltage gain is highest at low frequency (about 27 at 1 GHz) and rolls off monotonically to roughly 4–5 by 10 GHz. This behaviour reflects the transistor's finite transition frequency: parasitic capacitances

reduce transconductance and introduce additional phase shift as frequency increases. The measured DC bias currents are in line with those from Exercise 1, so the gain reduction is dominated by device high-frequency limits rather than a change in operating point.

6 Time-Domain Distortion and Antenna Performance (Lab 5)

Exercise 1: Time-domain non-linear distortion

The common-emitter amplifier was analysed in DC/AC to establish its operating point and small-signal gain, then simulated in transient with a swept input amplitude. At low drive levels the output is sinusoidal and scales linearly with the input. As the input amplitude is increased, the transistor leaves its linear region and the output exhibits clipping/compression, as shown in Fig. 14.

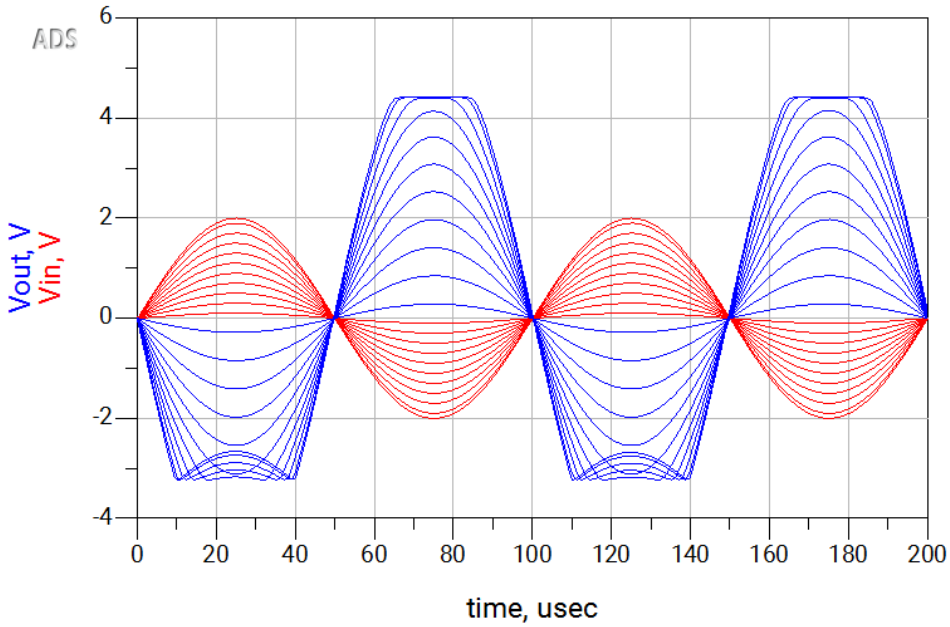

Figure 14: Transient input (red) and output (blue) waveforms for increasing input amplitude.

This distortion corresponds to the gain becoming signal-dependent. In the frequency domain a clipped sinusoid requires additional harmonic components to reconstruct the waveform, so harmonic balance would show rising harmonics and, for multi-tone inputs, intermodulation products. The onset of visible clipping therefore marks the practical linearity limit for the stage.

Exercise 2: Rectangular microstrip patch antenna

Using the FR4 substrate parameters ($\varepsilon_r = 4.6$, $h = 1.6$ mm) and a target resonance of $f_r = 2.4$ GHz, the patch dimensions follow from the design equations:

$$W = L = \frac{c}{2 f_r \sqrt{\varepsilon_r}} \approx 29.14 \text{ mm}, \qquad H = 0.822\,\frac{L}{2} \approx 11.98 \text{ mm},$$

$$Y = \frac{W}{5} \approx 5.83 \text{ mm}, \qquad X = Z = \frac{2W}{5} \approx 11.66 \text{ mm}.$$

The layout was implemented in ADS Momentum and simulated from 1–4 GHz.

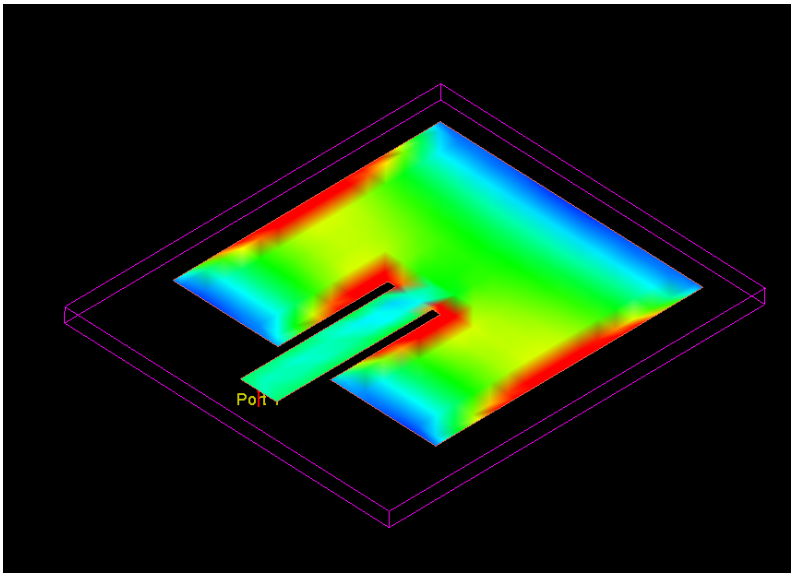

Figure 15: ADS layout of the 2.4 GHz rectangular patch antenna.

The simulated input match is shown in Fig. 16. A clear resonance occurs close to 2.4 GHz where S_{11} dips below -20 dB, confirming good impedance matching at the design frequency.

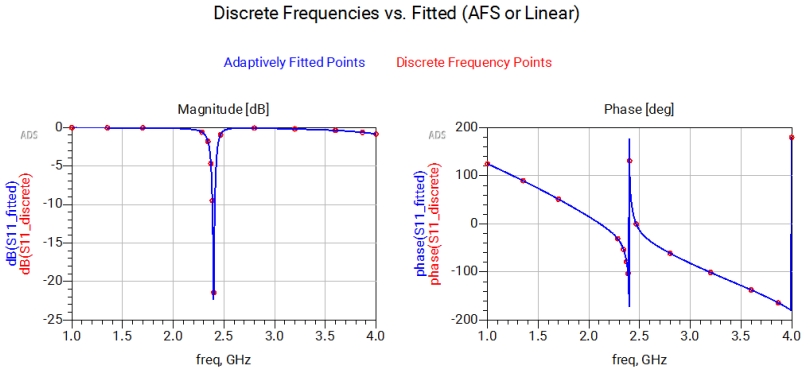

Figure 16: Simulated return loss S_{11} of the patch antenna.

Far-field results at 2.4 GHz are summarised in Fig. 17. The antenna radiates a broadside pattern with peak directivity of about 6.3 dBi and realised gain around 4.9 dBi, corresponding to roughly 73% efficiency. The polar cuts in the principal planes show the expected single-lobe behaviour for a rectangular patch and low cross-polarisation in the main beam.

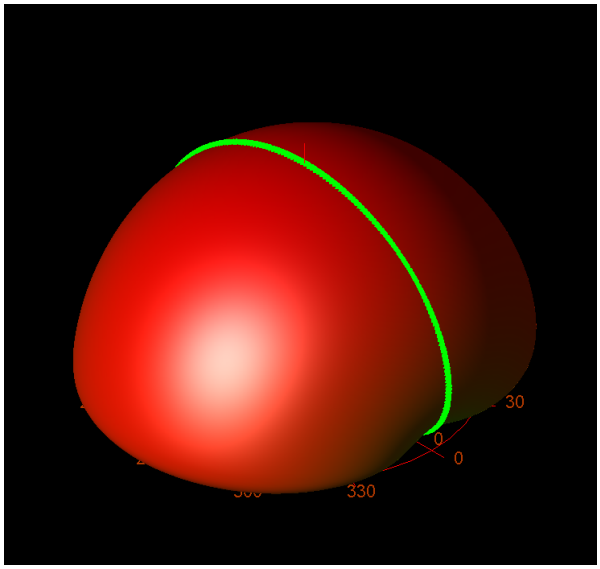

(a) Gain/directivity and efficiency.

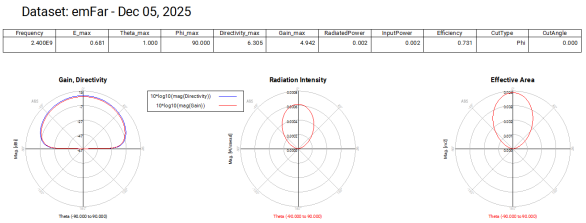

(b) Far-field cut (plane 1).

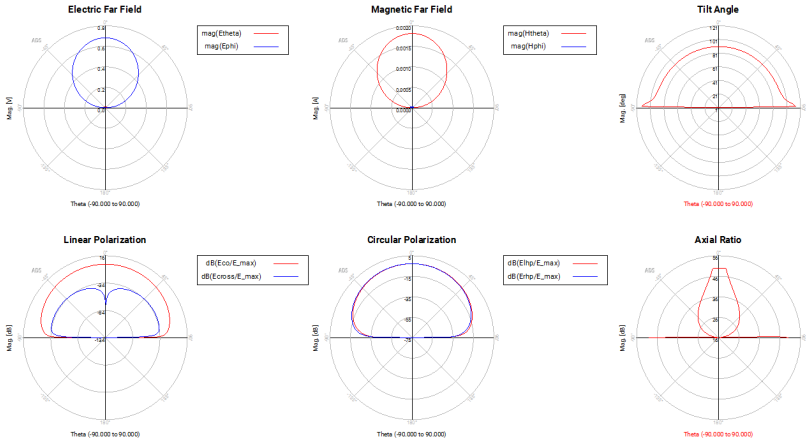

Figure 17: Simulated far-field characteristics of the patch antenna at 2.4 GHz.

7 Cross-Subsystem Discussion

- How link budget results define required amplifier gain and noise margin.
- How amplifier linearity and filter behaviour interact in a real chain.
- How device-level characteristics feed into system-level performance.
- Limitations of the simulations (ideal models, omitted noise sources, parasitics, EM simplifications).

8 Conclusion

- What was demonstrated,
- What was learned about subsystem behaviour,
- How the results relate to practical wireless system design.

Bibliography

[1] S. Robertson and Chongcheawchaman, *Microwave and Millimetre-Wave Design for Wireless Communications*. John Wiley & Sons, 2016.

[2] N. Somjit, "Elec5333m lecture 1 (link budget), slide 10," 2025.